Morphological Distribution of Polymeric Nucleating Agents in Injection-Molded Isotactic Polypropylene Plates and Its Influence on Nucleating Efficiency

Zhi-Qiang Su, Xiao-Nong Chen, Zhong-Zhen Yu, Liang Zhang

Key Laboratory of Beijing City on Preparation and Processing of Novel Polymer Materials, Beijing University of Chemical Technology, Beijing 100029, People's Republic of China

Received 4 June 2008; accepted 24 July 2008
DOI 10.1002/app.29098
Published online 13 October 2008 in Wiley InterScience (www.interscience.wiley.com).

ABSTRACT: The morphological development of a special polymeric nucleating agent [acrylonitrile–styrene copolymer (SAN)] in the isotactic polypropylene (iPP) matrix in the process of injection molding has been investigated by means of wide-angle X-ray diffraction and scanning electron microscope. The current experimental results indicate that the shear field, in combination with the temperature gradient, has great influence on the morphological distribution of SAN in the process of injection molding. For injection-molded SAN/iPP specimens with higher SAN concentration ($\geq$4%), SAN assembles to many microspheres and disperses uniformly in the isotropic core region; while from isotropic core region to oriented skin region, these SAN microspheres are gradually stretched into fibrils as a result of shear effect. On the contrary, for the specimens with lower SAN concentration (<4%), only microspheres can be observed in the core region and the skin region. At the same time, SAN has been proved to be a kind of special β-nucleating agent. The addition of SAN into iPP helps enhances the crystallinity and the content of β crystal form of injection-molded specimen. The morphology and the distribution of SAN in iPP matrix have great influence on the SAN's nucleating activity, which will ultimately affect the final crystalline structures of injection-molded specimens. © 2008 Wiley Periodicals, Inc. J Appl Polym Sci 111: 786–793, 2009

Key words: nucleation; morphology; shear; crystallization; polypropylene

INTRODUCTION

Processing and shaping operations of semicrystalline polymer materials, such as extrusion, injection molding, and fiber spinning, cause orientation and crystallization of polymer molecules in the melt, which strongly influence the final morphology and crystalline structure of the polymer.[1] In the process of injection molding of semicrystalline polymers, molten polymers are exposed to a temperature gradient and varying levels of a shear flow field prior to crystallization. The resulting morphology is thus quite different from what is observed under the quiescent condition. Especially, an oriented skin region and an isotropic core region can form in semicrystalline polymer plates during the operation of injection molding. Higher content of oriented texture induced by shear flowing can be preserved in the skin region because of rapid cooling, whereas the core region usually contains an isotropic texture, because the melt in the internal part of the mold cools down more slowly and the lower shear–strain history allows a complete relaxation of oriented texture.[2–9]

In industrial production, it is very common to add suitable nucleating agents into polypropylene during injection molding. Nucleating agents are used not only because they can significantly increase the crystallization rate of the molten polymers, but also because they would influence the crystalline structure of sheared polymers dramatically and selectively. As a result, the physical, mechanical, and optical properties of isotactic polypropylene (iPP) are improved. The addition of nucleating agent into iPP matrix in the process of injection molding will certainly complicate the crystallization process and the morphology that subsequently forms.[10–13]

Generally speaking, the β-nucleating agents of iPP are crystallizable organic compounds with low molecular weight.[14–18] Nevertheless, according to our investigation,[19] some polymers with benzene rings [such as acrylonitrile–styrene copolymer (SAN) and polystyrene (PS)] can also induce the β-iPP polymorph during quiescent isothermal crystallization and remarkably improve the impact strength of iPP. These polymeric nucleating agents, being different

Correspondence to: Z.-Q. Su (suzq@mail.buct.edu.cn).
Contract grant sponsor: National Natural Science Foundation of China (NSFC); contract grant number: 20704025.

from the traditional β-nucleating agents, present unique structural characteristics (both chain structure and condensed state structure) and nucleating activity. The assembled state (i.e., shape, size, and distribution) of polymeric nucleating agent (SAN) greatly influence the crystalline structure of iPP, which has direct effects on the properties and performance of products. Although the morphology of injection-molded semicrystalline polymers has been widely studied, much experimental work[6–9,20,21] is mainly devoted to the effects of processing conditions of shear flow on resulting crystalline structures and the mechanical properties of final products. Few of them paid attention to the special nucleating ability of some polymers (such as SAN) and the influence of the morphology of polymeric nucleating agents on their nucleating efficiency.

All our previous researches on polymeric nucleating agents are on the basis of quiescent isothermal crystallization, which is not the same with the practical production of polymer materials. In the injection-molding process, because of shear effect and temperature field, the changing pattern of the nucleating ability of polymeric nucleating agents with their concentration, morphology, and thermal history of processing is quite different from that of quiescent isothermal crystallization. The purpose of our research is to investigate the morphological distribution of polymeric nucleating agents in injection-molded iPP plates and further discuss the influence of the morphology of polymeric nucleating agents on their nucleating efficiency. Furthermore, based on our research of polymeric nucleating agents, a new material modification method is put forward in this work.

EXPERIMENTAL

Materials and specimens preparation

The matrix polymer used in this wok was commercial-grade iPP, S1003, with a melt flow index of 2.5 g/10 min, $M_w = 2.8 \times 10^5$ g/mol, and melting temperature of 165°C, produced by Yanshan Petroleum and Chemical Corp., China. The polymer nucleating agent (SAN) was obtained from Mitsubishi Plastics, Inc., Japan, with a melt flow index of 2.2 g/10 min. Compounding of iPP with SAN was produced using a corotating twin-screw extruder (China), operating at a melting temperature of 210°C. The compounds were blended at a screw speed of 25 rpm. SAN proportion in SAN/iPP blends were 1, 2, 3, 4, and 5% by weight. After pelletizing and drying, the resultant product (SAN/iPP blend) and neat iPP were injection-molded in a rectangular plate of dimensions 20 × 12 × 3 mm^3 with the aid of a Demag NC4 injection-molding machine (Germany). The molding conditions were as follows: melting temperature 200°C, holding pressure 250 bar, and holding time 3.8 s. In this work, the neat iPP specimen underwent the same process of twin-screw extruder.

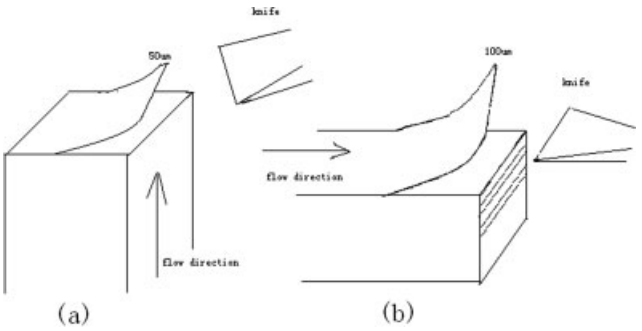

Scheme 1 Different microtomed methods for POM (a) and WAXD (b) measurements, respectively.

To observe the morphology of the injection-molded iPP specimens with the aid of POM, thin slices (~ 50 μm) were microtomed from the central part of specimen perpendicular to the flow direction [Scheme 1(a)]. The injection-molded iPP specimens were cut along the flow direction using a microtome, and the thin slices (about 100 μm) were used for wide-angle X-ray diffraction (WAXD) measurement for analyzing the crystalline structures of skin–core regions [Scheme 1(b)].

Measurements

WAXD experiments were conducted with a PaNalytical (Holland) X' pert Pro MRD diffractometer (Cu Kα, λ = 0.154 nm, 40 kV, 40 mA, reflection mode). The experiments were performed with a 2θ range of 10–30°, at a scanning rate of 2°/min and a scanning step of 0.02°.

Scanning electron microscope (SEM) measurements were carried out with a JSM-6700F SEM (JEOL, Japan). The injection-molded iPP specimens were first cryogenically fractured in liquid nitrogen along the flow direction. The morphology of fractured samples was observed by SEM.

For optical microscopy observation, a Nikon (Japan) type 104 optical microscope was used in this study. The optical microscope was equipped with cross-polarizer, with a camera system (Panasonic wv-CP240/G) incorporated.

The relative amount of different crystal forms presented in these specimens was measured from the X-ray diffraction profiles. In iPP WAXD profiles, (110) at 2θ = 14.1°, (040) at 16.9°, and (130) at 18.5° are the principal reflections of the α-crystal form of iPP, while (300) at about 15.9° is the principal reflection of the β-crystal form, and they are considered as the characteristic peaks for α-crystals and β-crystals, respectively. The crystallinity and relative

content of different crystal forms of iPP can be calculated from the following equations[22,23]:

$$K_\beta = \frac{A_{\beta(300)}}{A_{\alpha(110)} + A_{\alpha(040)} + A_{\alpha(130)} + A_{\beta(300)}} \quad (1)$$

$$X_{\text{all}} = 1 - \frac{A_{\text{amorphous}}}{\sum A_{\text{amorphous}} + A_{\text{crystallization}}} \quad (2)$$

where K_β expresses the relative amount of the β crystal form with respect to the α crystal form, $A_{\beta(300)}$ represents the area of the (300) reflection peak; $A_{\alpha(110)}$, $A_{\alpha(040)}$, and $A_{\alpha(130)}$ represent the areas of the (110), (040), (130) reflection peaks, respectively; $A_{\text{amorphous}}$ is the area of the amorphous phase. In this work, a curve-fitting software was used to calculate the peak intensities of WAXD profiles. The deconvoluted peaks can be obtained by using the mixed function of Gauss and Lorentz.

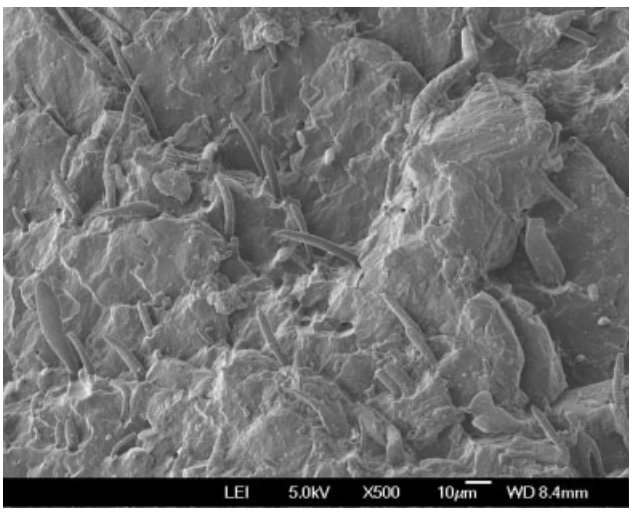

Figure 1 SEM microphotograph of the oriented skin region of the injection-molded SAN/iPP specimen; SAN proportion in the blend is 4% by weight.

RESULTS AND DISCUSSION

In our previous work,[19] we have proved that some polymers with benzene rings (such as SAN and PS) can induce the β-iPP polymorph during quiescent isothermal crystallization and improve the impact strength of iPP remarkably. At the same time, the nucleating activity of the polymeric nucleating agents showed significant dependence on their concentration, morphology, molecular structures, and crystallization temperature. To investigate the influence of shear effect on the morphology distribution of polymeric nucleating agent (SAN) in iPP matrix in the process of injection molding, SEM was used to observe the morphological distribution of SAN under shear flow in this work.

In this work, according to the difference of morphology distribution of SAN in iPP matrix, the injection-molded SAN/iPP plates were divided into three parts from surface to the internal part (i.e., oriented skin region, the transitional region, and isotropic core region). Figure 1 shows the SEM microphotograph of the oriented skin region of injection-molded SAN/iPP specimen. SAN proportion in the blend is 4% by weight and the flow direction is normal. Because of the phase separation between iPP and SAN, SAN usually disperses uniformly in iPP matrix, and the morphological distribution of SAN can be observed clearly by SEM. As shown in Figure 1, because of shear effect, SAN was stretched into many fibrils in the oriented skin region. These SAN fibrils disperse uniformly along the shear flowing direction.

Figure 2 shows the morphology distribution of SAN in the transitional region from oriented skin region to isotropic core region. The magnifying powers of Figure 2(a,b) are 500 and 1000, respectively. For SAN/iPP specimen with 4% SAN, the thickness range of the transitional region is about 300–1000 μm. It is obviously that, besides the stretched SAN fibrils, many SAN microspheres can also be observed in the transitional region [Fig. 2(a)]. Moreover, on further increasing the depth of the plate, the content of SAN microspheres increases gradually. The mixed morphology of fibrils and microspheres can be observed more clearly in the magnified SEM microphotograph of the transitional region in Figure 2(b). To distinguish the fibrils and microspheres in Figure 2(b), SAN microspheres were marked with circles, and the magnified photograph of SAN microspheres was pasted on the top right corner of Figure 2(b). The diameter of these microspheres was about 1 μm. The phenomena illustrate that, from the oriented skin region to the isotropic core region, the orientation degree of SAN/iPP specimen reduces gradually and some nonoriented SAN particles begin to aggregate into microspheres.

The SEM microphotographs of the isotropic core region of SAN/iPP plate with 4% SAN are provided in Figure 3 when the flow direction is normal. In the isotropic core region, there is almost no orientation in the middle of the injection-molded specimen and most SAN particles are aggregated into microspheres [Fig. 3(a)]. These microspheres are magnified in Figure 3(b). The diameter of these SAN microspheres in the isotropic core region almost equals to that in the transitional region. Furthermore, the transitional morphology from microsphere to fibril is observed and marked with a circle in Figure 3(a). It is apparent that the size of SAN particles in the transitional region (about 5 μm) is bigger than that of other SAN microspheres (about 1 μm). Therefore, in the process of injection molding, it is much easier

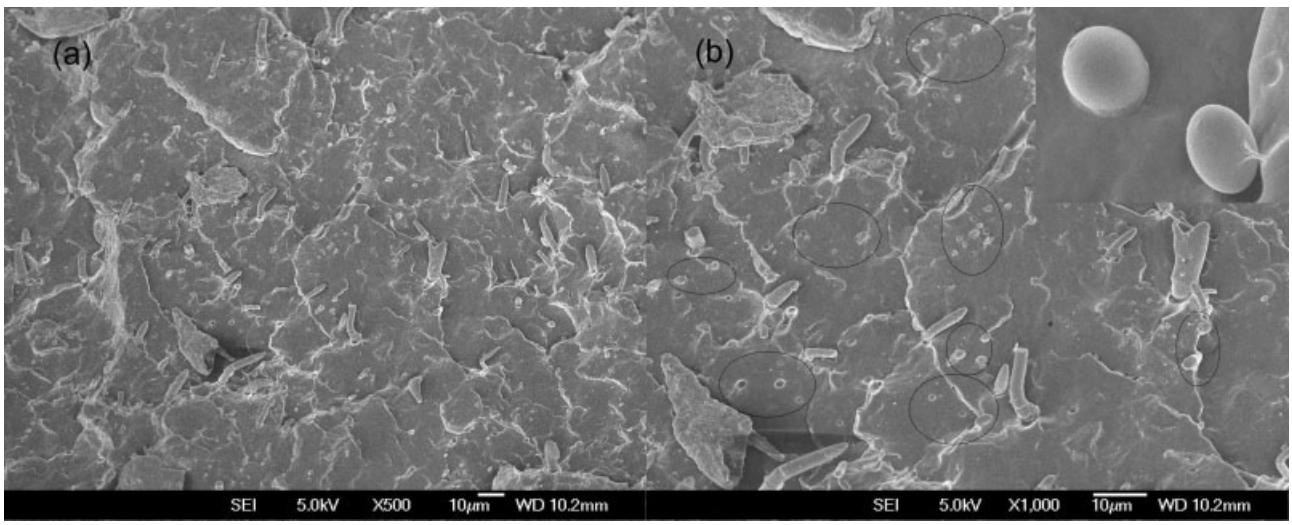

Figure 2 SEM microphotographs of the transitional region of the SAN/iPP specimen with 4% SAN. Magnifying power: (a) 500; (b) 1000.

for the bigger SAN microspheres to be stretched into fibrils.

All the earlier analysis and discussion clearly indicate that shear effect gradually decrease with the increase in the depth of the plate, which results in the changed morphology distribution of polymeric nucleating agent in the specimen.

According to SEM microphotographs of SAN/iPP specimens with higher SAN concentration (4%), we proposed a model to describe the morphology distribution of polymeric nucleating agent in iPP matrix during injection molding. Scheme 2 is the morphology distribution model of SAN from oriented skin region to isotropic core region. With the help of the model, we can better understand the changing pattern of SAN's morphology during injection molding.

In this work, we also investigate the morphology distribution of SAN in SAN/iPP injection-molded plate with different SAN concentration. For the mixture with higher SAN concentration (5%), the morphology distribution of polymeric nucleating agents is similar to the specimen with 4% SAN. In this case, SAN assembles to become microspheres and disperses uniformly in the isotropic core region, while these microspheres are gradually stretched into fibrils from isotropic core region to oriented skin region as a result of shear effect. On the contrary, for injection-molded SAN/iPP specimens with lower SAN concentration (1, 2, and 3%), SAN shows different morphological distribution in the iPP matrix.

Figure 4 shows the SEM microphotographs of isotropic core region (a) and oriented skin region (b) of

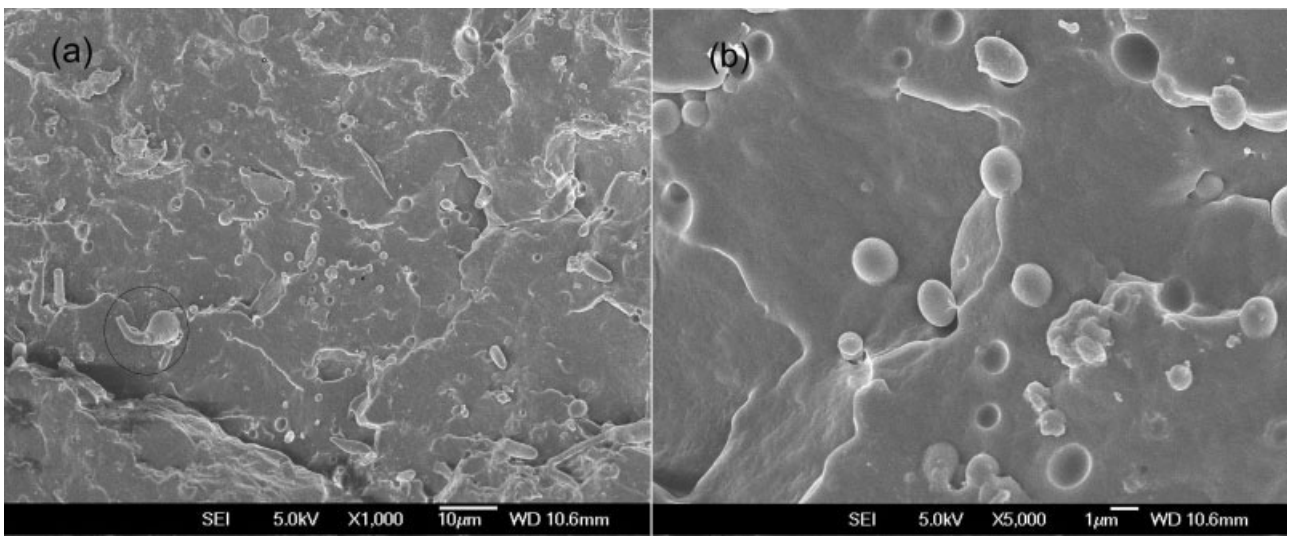

Figure 3 SEM microphotographs of the isotropic core region of iPP plate nucleated with 4 wt % SAN. Magnifying power: (a) 1000; (b) 5000.

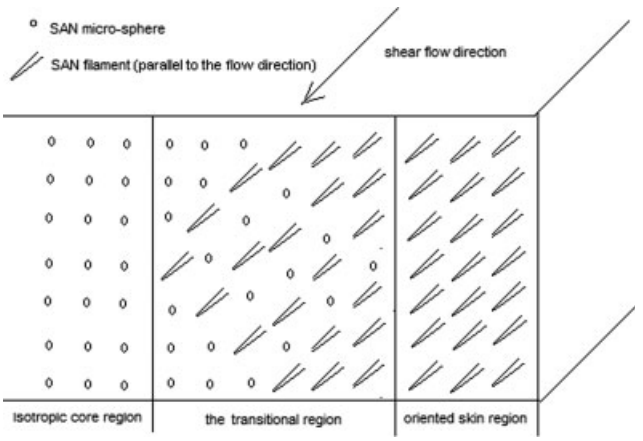

Scheme 2 The morphology distribution model of SAN in iPP matrix during injection molding. The content of SAN fibrils decreases with the increase in the depth of the plate, indicating the gradually decreasing shear effect.

the injection-molded SAN/iPP specimen with lower SAN concentration (3%). It is obvious that, in both the core and skin regions, only SAN microspheres can be observed. These microspheres disperse uniformly in the iPP matrix and the size of SAN microspheres does not change significantly (about 1 μm), indicating that the dispersion of SAN is good. Combined with the earlier analysis and discussion, we can deduce that the shear flowing has no effect on the morphology of the small-sized SAN microspheres in the process of injection molding.

As mentioned earlier, SAN has significant β nucleating effect on iPP. Typically, the morphology and the dispersion of SAN in iPP matrix have great influence on its nucleating efficiency. In the process of quiescent isothermal crystallization, SAN particles always aggregate into microspheres in iPP matrix, because there is no shear effect in processing operation. The size of SAN microspheres increases with the increase of SAN content and ultimately leads to a reduction of the nucleating activity of SAN.[19] In this work, the specimens were made by injection molding and some SAN was stretched into fibrils in the processing operation. The difference of morphology distribution of SAN between the skin and core region will also influence the crystalline structures of iPP. For a thorough study, WAXD was adopted to investigate the crystalline structures in different shear regions of the injection-molding specimen.

Figures 5 and 6 show the WAXD profiles in different shear regions of neat iPP and SAN/iPP specimens. SAN proportion is 4% by weight. To compare the crystalline structures of different specimens, the WAXD profiles were all plotted at the same intensity scale. Five obvious peaks at 2θ of approximate values 14.2°, 17.0°, 18.7°, 21.3°, and 22.0° correspond to the (110), (040), (130), (131), and (111) reflections of α crystal form of iPP, respectively, and an obvious peak at about 15.9° corresponds to the (300) reflection of β crystal form. During quiescent isothermal crystallization, the predominant crystal structure in neat iPP is always the α form, and the β form occurs rarely. However, there is a typical β peak at about 15.9° in some WAXD profiles of neat iPP plate (in Fig. 5), indicating that shear effect in injection molding helps produce a β crystal form. WAXD profiles of SAN/iPP specimen are well consistent with the corresponding one of neat iPP, while the reflection intensities of β peak is stronger than those of neat iPP given the same depth, indicating that SAN contributes to the increment of β-phase content in iPP.

According to the eqs. (1) and (2), the relative content of β crystal form (K_b) and the value of the total

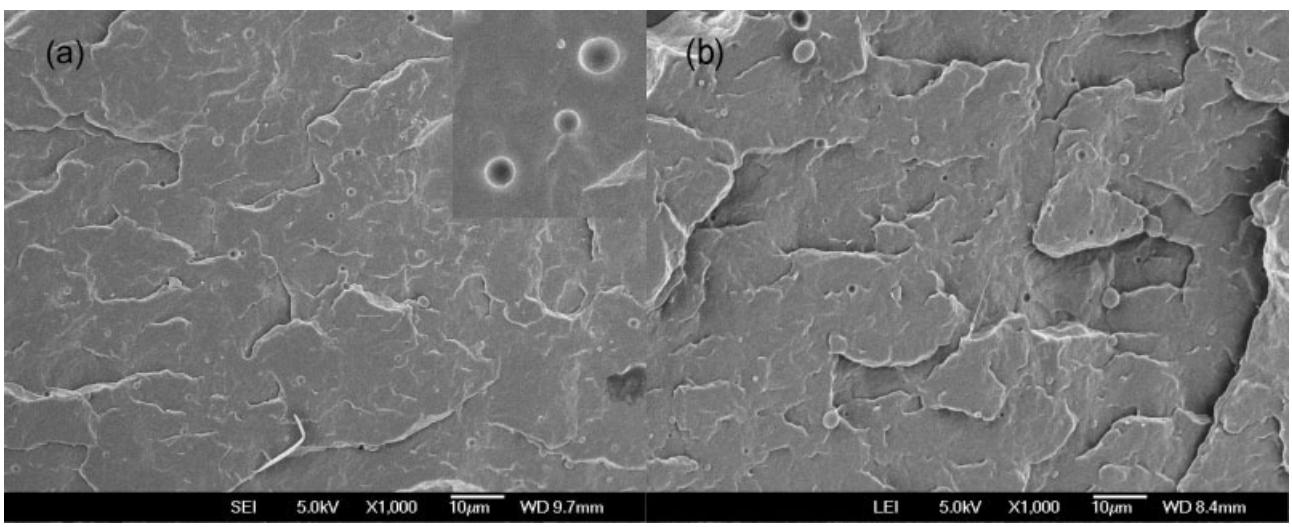

Figure 4 SEM microphotographs of isotropic core region (a) and oriented skin region (b) of SAN/iPP specimen with lower SAN concentration (3%).

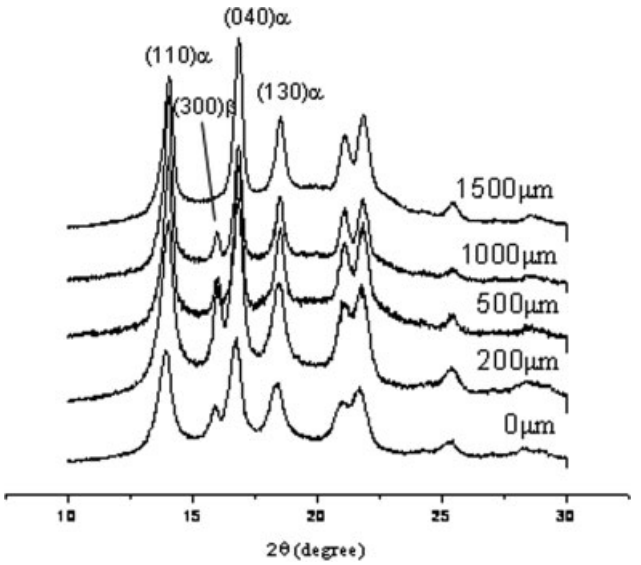

Figure 5 WAXD profiles of injection-molded neat iPP specimen. The number of each trace indicates the distance from the plate surface.

crystallinity (X_{all}), calculated from the X-ray diffraction profiles as shown in Figures 5 and 6, are reported in Figure 7 as a function of the distance from the surface of injection-molded specimen.

The calculated results show that the X_{all} values of the two series of specimens first increase with the increase in the depths of the plate, reach a maximum value (when the depth is about 200 μm), and then decrease with the further increase of depths. This can be attributed to the competitive effect of shear flowing and temperature gradient. Higher shear level and slower cooling rate favor high degrees of overall crystallinity. However, in the process of injection molding, from the skin to core region, both the shear effect and the cooling rate of temperature decrease gradually, which will result in the nonlinear change of the X_{all} values with the increase in the depths of the specimens.

Furthermore, the X_{all} values of SAN/iPP are bigger than those of neat iPP either in the skin region or in the core region. As for both series of specimens, iPP should crystallize in the same temperature gradient and shear field in the same depth. The difference in the X_{all} values of neat iPP and SAN/iPP specimen can only be explained by the addition of the polymeric nucleating agent into iPP matrix. The incorporation of SAN into the polymer matrix can promote iPP's nucleation and crystallization. As a result, higher crystallinity can be expected.

The changing patterns of K_b value of two series of specimens with the depths of injection-molded plates were also illustrated in Figure 7. It is apparent that, for both neat iPP and SAN/iPP plates, the K_b value has a maximum value in sheared skin region (the depth is about 200 μm) and gradually decreases with a deeper distance. It indicates that shear effect does display an obvious influence on enhancing the content of β crystal form. Furthermore, compared with neat iPP, the K_β values of SAN/iPP are larger than that of neat iPP in equal depth of injection-molded plates. Typically, in the core region, the reflection peak of β crystal form of neat iPP is absent, which is still discernable in the WAXD profiles of SAN/iPP specimen. These results further confirm the β nucleating effect of SAN in injection molding.

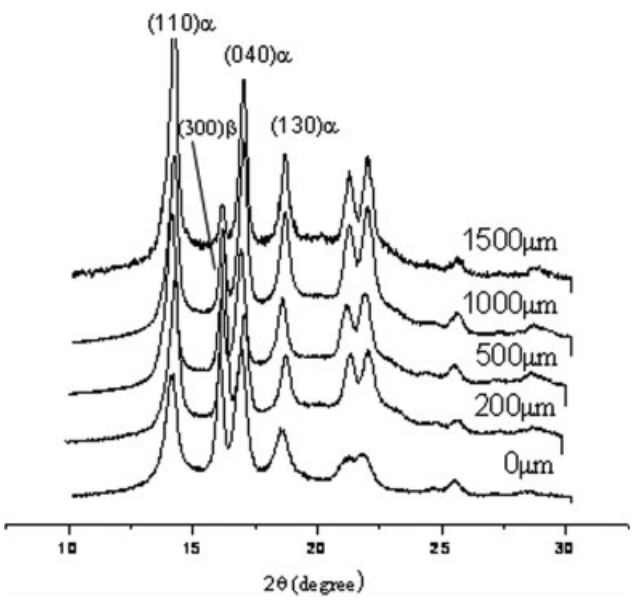

Figure 6 WAXD profiles of injection-molded SAN/iPP specimen (SAN% is 4%). The number of each trace indicates the distance from the plate surface.

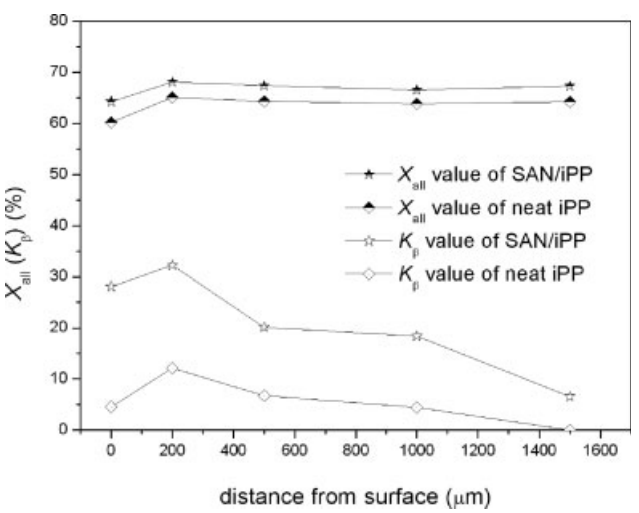

Figure 7 The relative content of β crystal form (K_β) and the value of crystallinity (X_{all}) as a function of distance from surface, evaluated from the X-ray diffraction patterns in Figures 5 and 6.

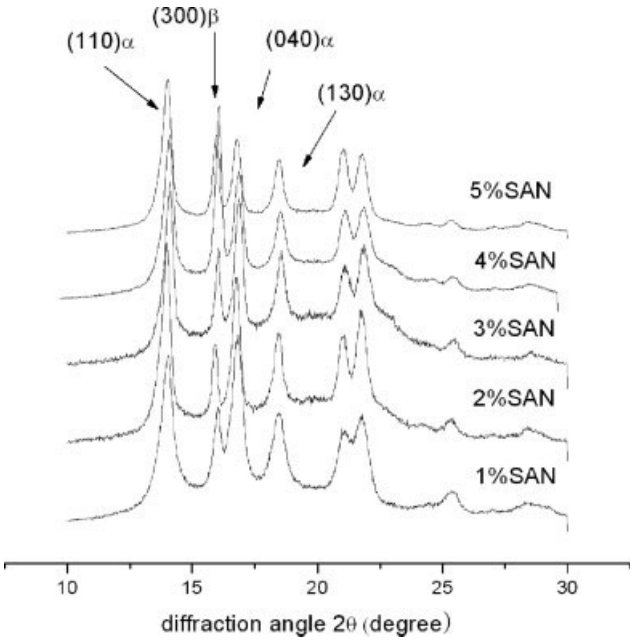

Figure 8 WAXD profiles in the skin region of injection-molded SAN/iPP specimens with different SAN concentration.

Comparing the WAXD curves in Figure 6, though shear effect has a great influence on the crystalline structure of injection-molded plates, it is apparent that the K_b value in the skin region (about 33%) is far greater than that in the core region (about 7%). The difference in the K_b values between the skin region and core region could not be explained only by shear effect during injection molding, as the morphology distribution of polymeric nucleating agent in iPP matrix may also play an important role. According to our previous investigation,[19] the morphology distribution of polymeric nucleating agent in iPP matrix has great influence on its nucleating efficiency. Increasing the specific surface of polymeric nucleating agent and improving its dispersibility in iPP matrix will improve the β nucleating efficiency of the polymeric nucleating agent.

Through SEM, we have found out that the morphology distribution of SAN in the skin and core region is completely different. Most of the SAN were stretched into fibrils in the oriented skin region, while they aggregated into microspheres in the core region. When microspheres were stretched into fibrils, they get bigger specific surface area and better dispersibility, which will finally promote the β nucleating efficiency of SAN. To further confirm the influence of the morphology of SAN on its nucleating efficiency, we also compared the K_b value of iPP/SAN plates with different SAN concentrations.

Figure 8 shows the WAXD profiles in skin region of injection-molded SAN/iPP specimens with different SAN concentrations. The proportion of SAN is 1, 2, 3, 4, and 5% by weight, respectively. The changing pattern of the relative content of β crystal form (K_b) with the change of SAN concentration is reported in Figure 9. It is obvious that, as SAN concentration increases from 3 to 4%, the K_b value of iPP/SAN sample increases rapidly and greatly. According to the earlier discussion, 3–4 wt % of SAN in iPP matrix is the critical range for the morphology distribution of SAN to occur (extended fibril in skin region, mixture of fibril and spheres in the transition region, and microspheres in the isotropic core region). For iPP/SAN (3 wt%) specimen, shear flow has no effect on the morphology of SAN in the process of injection molding, and only small size microspheres can be observed in both the core and the skin region. While SAN microspheres are stretched into fibrils in skin region when SAN concentration is higher than 4%. It is known that SAN fibrils have bigger specific surface and better dispersibility than SAN microspheres, and thus can remarkably enhance the nucleating efficiency of SAN. Therefore, the rapid increase of K_b value in iPP/SAN (4 wt%) can be explained by the difference of SAN's morphology and distribution. An interesting phenomenon is that, the K_b values of iPP/SAN samples decrease when the SAN concentration increases from 4 to 5%. It can be attributed to the decrease of the dispersibility of SAN in iPP matrix with further increase of SAN concentration.

In the traditional process of material modification, a large amount of modified polymers (such as PS, PA, PE, SAN, etc) were added into iPP to improve the mechanical properties of iPP by blending modification. In fact, according to our experience, the effect of blending modification is limited because of the bad miscibility and the phase separation among

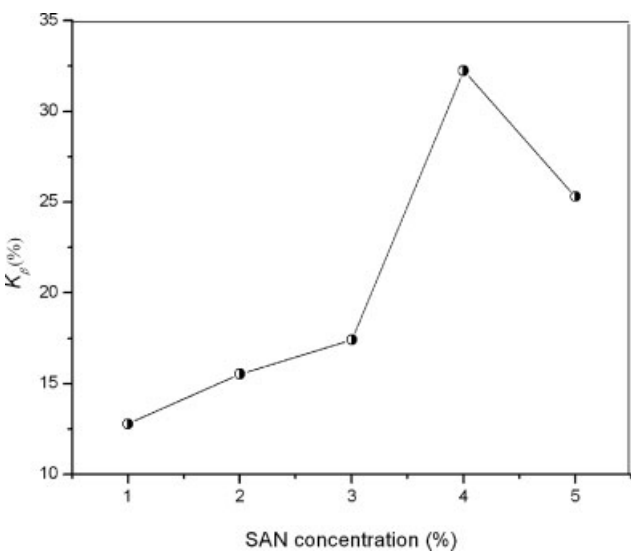

Figure 9 The relative content of β crystal form (K_β) as a function of SAN concentration, evaluated from the X-ray diffraction patterns in Figure 8.

different blending polymers. Based on our research of polymeric nulceating agent, a new material modification method was put forward, that is to reduce the content of the modified polymers greatly in the process of traditional blending modification (these modified polymers should have significant nucleating ability) and to control the crystalline structure and properties of iPP by these modified polymers. In this material-modified process, the dispersibility of modified polymers was improved greatly and the mechanical properties of blending materials were enhanced significantly.

Through comparing the mechanical ability data (including stretching, bending, impact strength) of pure iPP and SAN/iPP samples, it was found that the impact strength of SAN/iPP was obviously improved than that of pure iPP. When SAN percentage is 4%, the maximum impact strength value of SAN/iPP can be enhanced by almost 70%. At the same time, these polymeric nucleating agents have many excellent performances (such as cheapness, innocuity, easy to process) and exhibit an attractive commercial future.

CONCLUSIONS

The morphological development of a special polymeric nucleating agent (SAN) in iPP matrix in the process of injection molding has been investigated in the current study. The following conclusions can be drawn:

With the help of SEM, it was found that the shear flowing has great influence on the morphological distribution of SAN in iPP matrix in the process of injection molding. For the injection-molded SAN/iPP specimens with higher SAN concentration ($\geq$4%), the shear effect decreased gradually from the skin region to the core region. Most of the SAN were stretched into fibrils in the oriented skin region, while some SAN began to aggregate into microspheres with the increase in the depths of the injection-molded plates. On the contrary, for the injection-molded SAN/iPP specimens with lower SAN concentration ($<$4%), only SAN microspheres can be observed in both the core and the skin region.

WAXD results indicate that SAN has significant nucleating effect on iPP in the process of injection molding. The morphological distribution of SAN in iPP matrix has great influence on its nucleating efficiency, which ultimately influences the crystalline structure of the injection-molded specimen. Furthermore, based on our research of polymeric nucleating agents, a new material modification method was put forward in this work.

References

1. Agarwal, P. K.; Somani, R. H.; Weng, W. Q.; Mehta, A.; Yang, L.; Ran, S. F.; Liu, L. Z.; Hsiao, B. S. Macromolecules 2003, 36, 5226.
2. Ulcer, Y.; Cakmak, M. Polymer 1997, 38, 2907.
3. Schrauwen, B. A. G.; Breemen, L. C. A.; Spoelstra, A. B.; Govaert, L. E.; Peters, G. W. M.; Meijer, H. E. H. Macromolecules 2004, 37, 8618.
4. Viana, J. C. Polymer 2004, 45, 993.
5. Clark, E. S.; Spruiell, J. E. Polym Eng Sci 1976, 16, 176.
6. Sousa, R. A.; Reis, R. L.; Cunha, A. M.; Bevis, M. J. J Appl Polym Sci 2003, 2079, 89.
7. Fujiyama, M.; Wakino, T.; Kawasaki, Y. J Appl Polym Sci 1988, 35, 29.
8. Choi, D.; White, J. L. Polym Eng Sci 2002, 42, 1642.
9. Zhu, P. W.; Tung, J.; Phillips, A.; Edward, G. Macromolecules 2006, 39, 1821.
10. Blomenhofer, M.; Ganzleben, S.; Hanft, D.; Schmidt, H.; Kristiansen, M.; Smith, P.; Stroll, K.; Mader, D.; Hoffmann, K. Macromolecules 2005, 38, 3688.
11. Jang, G.; Cho, W.; Ha, C. J Polym Sci Part B: Polym Phys 2001, 39, 1001.
12. Reguera, D.; Rubi, J. M. J Chem Phys 2003, 119, 9877.
13. Nogales, A.; Mitchell, G. R.; Vaughan, A. S. Macromolecules 2003, 36, 4898.
14. Chen, H. B.; Karger, K. J.; Wu, J. S.; Varga, J. Polymer 2002, 43, 6505.
15. Lotz, B. Polymer 1998, 39, 4561.
16. Stocker, W.; Schumacher, M.; Graff, S.; Thierry, A.; Wittmann, J. C.; Lotz, B. Macromolecules 1998, 31, 807.
17. Wittmann, J. C.; Lotz, B. Prog Polym Sci 1990, 15, 909.
18. Mathieu, C.; Thierry, A.; Wittmann, J. C.; Lotz, B. Polymer 2000, 41, 7241.
19. Su, Z. Q.; Dong, M.; Guo, Z. X.; Yu, J. Macromolecules 2007, 40, 4217.
20. Somani, R. H.; Yang, L.; Hsiao, B. S.; Agarwal, P. K.; Fruitwala, H. A.; Tsou, A. H. Macromolecules 2002, 35, 9096.
21. Eder, G.; Janeschitz, K. H. Colloid Polym Sci 1988, 266, 1087.
22. Somani, R. H.; Hsiao, B. S.; Nogales, A.; Fruitwala, H.; Srinivas, S.; Tsou, A. H. Macromolecules 2001, 34, 5902.
23. Huo, H.; Jiang, S. C.; An, L. J.; Feng, J. C. Macromolecules 2004, 37, 2478.